

**COOLING STRATEGIES OF LITHIUM-ION BATTERIES USING
AIR**

ALVIN LEON ANJIE ANAK PENGUANG

**CHEMICAL ENGINEERING
UNIVERSITI TEKNOLOGI PETRONAS
JANUARY 2021**

Cooling Strategies Of Lithium-Ion Batteries Using Air

by

Alvin Leon Anjie Anak Penguang

24443

Dissertation submitted in partial fulfilment of
the requirements for the
Bachelor of Engineering (Hons)
(Chemical Engineering)

JANUARY 2021

Universiti Teknologi PETRONAS,
32610, Bandar Seri Iskandar,
Perak Darul Ridzuan

CERTIFICATION OF APPROVAL

Cooling Strategies Of Lithium-Ion Batteries Using Air

by

Alvin Leon Anjie Anak Penguang

24443

A dissertation submitted to the
Chemical Engineering Programme
Universiti Teknologi PETRONAS
in partial fulfilment of the requirement for the
BACHELOR OF ENGINEERING (Hons)
(CHEMICAL ENGINEERING)

Approved by,

(Dr. Mohd. Hilmi B. Noh)

UNIVERSITI TEKNOLOGI PETRONAS
BANDAR SERI ISKANDAR, PERAK
JANUARY 2021

CERTIFICATION OF ORIGINALITY

This is to certify that I am responsible for the work submitted in this project, that the original work is my own except as specified in the references and acknowledgements, and that the original work contained herein have not been undertaken or done by unspecified sources or persons.



ALVIN LEON ANJIE ANAK PENGUANG

ABSTRACT

The popular green power will become the light of the future especially with the rising numbers of electric cars produced. The electric cars were powered up using lithium-ion batteries as they are high in power and energy density and capable to be recharged many times. However, the working mechanism of the lithium-ion batteries generates heat which is extremely dangerous if not being controlled. Therefore, this particular research paper explains on the cooling strategies of lithium-ion batteries. The objectives of this paper are to study the impact of air flow to cool down lithium-ion battery pack and to evaluate important parameters which affect air cooling effectiveness. The scope of study covers the study of the air-cooling parameters such as battery layout analysis, distance between the battery cells, air inlet and outlet sizing, type of air flow and the velocity of air. The parameters were studied by using COMSOL Multiphysics 5.4 which utilizes heat transfer in solids and liquid and two different flow which are laminar and turbulent flow. The simulation was a success due to the manipulated parameters, the hot working lithium-ion batteries of 350 K were able to be cooled down to their safe optimum operating temperature of 295.47 K. The best battery layout analysis obtained is 3S3P with a 0.003 m of distance between each battery followed by inlet and outlet sizing of 0.065 m. The type of flow best suited the cooling strategies is laminar flow with the speed of 10 m/s. Therefore, the best cooling strategies of lithium-ion batteries using air can be obtained from this paper.

ACKNOWLEDGEMENTS

I would like to express my sincerest gratitude to my Final Year Project supervisor, Dr. M. Hilmi B Noh for his unparalleled support and gave me the golden opportunity to do this project on the topic of the Cooling Strategies of Lithium-Ion Batteries. His invaluable insight and unwavering guidance have helped me to do my research better and achieve the objectives of my project. I am very grateful to him, for his trust in my abilities and aptitudes for the past few months. In addition, I appreciate Dr. Hilmi's efforts to lead the direction and sharing experience with me which has urged myself to be increasingly autonomous and determined to do my job better. His ability to willingly spent their time and helping both objectively and profoundly has been specially valued. I would also like to express my gratitude to Dr. Azella for her practical suggestions during the progress assessment question and answer session.

Last but not least, I must express my profound gratitude to my family for their unfailing support and encouragement throughout my final year journey. This accomplishment would not have been possible without them.

TABLE OF CONTENTS

CERTIFICATION OF APPROVAL	ii
CERTIFICATION OF ORIGINALITY	iii
ABSTRACT	iv
ACKNOWLEDGEMENTS	v
LIST OF FIGURES	viii
LIST OF TABLES	ix
CHAPTER 1: INTRODUCTION	1
1.1 Background	1
1.2 Problem Statement	2
1.3 Objectives	3
1.4 Scope of Study	4
CHAPTER 2: LITERATURE REVIEW	5
CHAPTER 3: METHODOLOGY	11
3.1 Comparison of Research Method	12
3.2 Project's Modelling Methodology	13
3.3 COMSOL Multiphysics 5.4 Software	13
3.3.1 Heat Transfer in Solids and Fluids	14
3.3.2 Laminar Flow	14
3.3.3 Turbulent Flow	14
3.4 Properties of Lithium-Ion Batteries	15
3.5 Properties of Air	15
3.6 Boundary and Initial Condition	16
3.7 Meshing Numerical Scheme	17
CHAPTER 4: RESULT AND DISCUSSION	20
4.1 Battery Layout Analysis	20
4.2 Distance Between Battery Cells	23
4.3 Air Inlet and Outlet Sizing	24

4.4	Type of Air Flow	25
4.5	Velocity of Air	26
4.6	Best Cooling Strategies	27
CHAPTER 5:	CONCLUSION AND RECOMMENDATION	28
5.1	Conclusion	28
5.2	Recommendation	29
REFERENCES		30
APPENDICES		33

LIST OF FIGURES

Figure 2.1	Components inside lithium-ion batteries (Samsung,2016)	7
Figure 2.2	Lithium-ion batteries (Samsung,2016).	8
Figure 2.3	Degradation mechanisms inside lithium-ion batteries (Birkel, Roberts, McTurk, Bruce & Howey,2017)	9
Figure 2.4	Air cooling battery thermal management system (Quesnel, 2018)	10
Figure 3.1	Simulation methodology flowchart	11
Figure 3.2	3D simulation model	17
Figure 3.3	Temperature evolution along the x-axis for all types of meshes	18
Figure 3.4	Fine mesh simulation model	19
Figure 4.1	3S3P batteries layout	21
Figure 4.2	9S batteries layout	21
Figure 4.3	Temperature distribution in 3S3P batteries	22
Figure 4.4	Temperature distribution in 9S batteries layout	22
Figure 4.5	Temperature difference for 3S3P and 9S batteries layout	23
Figure 4.6	Temperature vs Distance between the batteries graph	24
Figure 4.7	Temperature distribution for 0.003 m distance between the battery cells	25
Figure 4.8	Plot of the middle row's batteries	26
Figure 4.9	Temperature of the second row of battery pack for different distance between batteries	26
Figure 4.10	Temperature vs Air inlet and outlet sizing graph	27
Figure 4.11	Temperature difference for laminar and turbulent flow	29
Figure 4.12	Temperature vs Velocity of air graph	30
Figure 4.13	Temperature of the second row of battery pack for different velocity of air	31

LIST OF TABLES

Table 3.1	Comparison of research method	12
Table 3.2	Properties of lithium-ion batteries	15
Table 3.3	Properties of air	16
Table 3.4	Design properties and parameters of 3D model	17
Table 4.1	Temperature distribution for 3S3P and 9S batteries layout	23
Table 4.2	Temperature distribution for different distance between the battery cells	23
Table 4.3	Temperature distribution for different air inlet and outlet sizing	25
Table 4.4	Temperature distribution for different type of air flow	26
Table 4.5	Temperature distribution for different velocity of air	26
Table 4.6	Parameter's properties for the best cooling strategies	27

CHAPTER 1

INTRODUCTION

1.1 Background

One of the most pressing social problems of this decade is global warming. In the future, global warming will have even more negative effects for natural ecosystems and human communities (Geest, et al., 2018). Reliance on fossil fuels, especially for transportation, increases greenhouse gas emissions, which are a major contributor to global warming (Global Warming FAQ, 2008). Internal combustion engines are the key component of the transportation sector that contributes to this problem by emitting carbon dioxide (Sharaf, 2013). Internal combustion engines are undesirable because of their detrimental effects on air quality, human health, and, most importantly, global warming (Sharaf, 2013). As a result, as environmental rules on greenhouse gas emissions have been strengthened, interest in electric cars (EV) has grown considerably (Kim, Oh, & Lee, 2019).

However, finding an adequate energy storage system that can support high mileage, rapid charging, and high driving performance is the basic issue that EVs faced (Dunn, Kamath, & Tarascon, 2011). Due to their high energy density and power density, lighter weight, lower self-discharge rates, and longer life cycle than other recyclable batteries such as lead-acid and nickel-cadmium, rechargeable lithium-ion batteries are considered as the best energy storage medium for EVs thanks to updated technology and research (Tarascon & Armand, 2010). Another benefit of using a lithium-ion battery (LIB), according to Sasaki, Ukyo, and Novak (2013), is that the cell has no memory effect.

Nevertheless, the performance, life cycle and safety aspect of these lithium-ion batteries are very sensitive to temperature. (Bandhauer, Garimella, & Fuller, 2011). Based on the research done by Thomas and Newman (2003), heat is generated in battery cell due to the reversible entropy, resistive dissipation, relaxation of the concentration gradient of the cell and chemical reaction. Generated heat must be eliminated quickly to avoid the degradation of the battery in terms of safety and performance aspects thus proper designed battery cooling strategies are required to increase the lifetime of lithium-ion cell.

1.2 Problem Statement

One of the major limitations of the application of lithium-ion batteries (LIB) in electric vehicles is the impact of temperature to the proper operating condition of the cell. The lithium-ion batteries' optimal temperature is within the range of 288.15 K to 308.15°C (Pesaran, Santhanagopalan, & Kim, 2013). If the temperature of the batteries is out of these regions, the batteries will degrade faster with an increased risk of facing safety problems such as fire and explosion (Ma, et al., 2018).

At a low operating temperature, the lithium-ion batteries will show slow chemical reaction activity and charge-transfer velocity, which leads to the reduction of ionic conductivity in the electrolytes and lithium-ion diffusivity within the electrodes (Ma, et al., 2018). In contrast, higher temperature will degrade the performance of the batteries including the formation of solid electrolytes interphase on the electrodes, loss of capacity and power and if the temperature is out of control, thermal runaway can be triggered which will lead to self-ignition and explosion (Wang, et al., 2012). However, the high temperature effects are more likely to happen and can be seen in a broad range of applications which includes in both low and high temperature environments.

As a result of the negative impacts of high temperature on the batteries, cooling strategies are required to dissipate the heat thus maintaining the proper temperature range and minimizing the temperature gradient of these batteries. There are several

cooling mediums used which had been investigated namely air cooling, liquid cooling and phase change material cooling system (Qian, Li, & Rao, 2016). However, air cooling is still the better choice due to its advantages of structure simplicity, light weight, low cost and has a good cooling performance as compared to its competitors (Wang & L.Ma, 2017).

In order for the strategies to work well, a proper designed of air-cooling strategies is studied. Parameters such as battery layout analysis in a pack, distance between battery cells, air inlet and outlet sizing, characteristic of air flow namely the type of flow and velocity of air are being determined to build a well-functioning cooling system which is capable to prevent thermal runaway, loss of capacity and maximize cell lifespan.

1.3 Objectives

This research focuses on the air-cooling strategies of working 18650 lithium-ion batteries (LIB) to mitigate heat generated. Heat generated will degrade the cells' performance and introducing safety concern due to the thermal effect towards the batteries. The main cooling medium selected is air due to its many advantages compared to the other cooling medium. Parameters which affect the cooling performance will be studied to keep batteries in its optimal operating temperature.

This research focuses on two main objectives which are as follow:

- i. To study the impact of air flow to cool down lithium-ion battery pack
- ii. To evaluate important parameters which affect air cooling effectiveness

1.4 Scope of Study

The main simulation and modelling software being utilized in this research is COMSOL Multiphysics 5.4. The design of the cooling strategies will be simulated to meet the requirement of an effective cooling performance. To maximize the cooling capacity, several parameters will be studied to boost the cooling efficiency. Good lithium-ion batteries cooling strategies will reduce the detrimental effects of high temperature and maintain the great performance of lithium-ion batteries (Ma, et al., 2018).

The scope of study in this particular research covers the following aspects:

- i. Battery layout analysis
- ii. Distance between the battery cells
- iii. Air inlet and outlet sizing
- iv. Type of air flow
- v. Velocity of air

CHAPTER 2

LITERATURE REVIEW

Electricity generated in a more environmentally friendly manner is referred to as green power (Rowlands, Parker, & Scott, 2002). Green power has been steadily increasing in popularity as a viable alternative to fossil fuels in recent years. It has attracted global attention and is being quickly designed to address the unrenewable energy crisis as well as environmental issues such as global warming. According to Rahman (2003), electricity generated from renewable energy sources is regarded as "green" because it has a low effect on greenhouse gas emissions. Renewable energy resources such as wind farms, geothermal projects, biomass projects, photovoltaic solar panels, and others are also used to generate green power (Zarnikau, 2003). Renewable energy technologies have a greater share of the electricity generation mix in order to minimize the dependence on oil and the emission of carbon dioxide. Energy from electrochemical batteries is also considered as green power due to no emission of pollutants to the environment (Nanaki & J.Koroneos, 2013).

The history of electrochemical batteries was originated by Alessandro Volta, who invented the first electrochemical batteries back in 1800 and since then has become the one of the basic necessities in human's life. (Bagotsky, 2011). Electrochemical batteries are classified into primary and secondary batteries. Primary batteries are only used once and cannot be recharged due to its irreversible electrochemical reaction (Ma, et al., 2018). Some example of primary batteries is zinc-carbon batteries. On the other hand, secondary batteries are rechargeable batteries which can be cyclically be reused by discharging and recharging. Among all the different types of secondary batteries, lithium-ion batteries (LIB) are one of the most popular battery and are widely used in many areas. Sony Corporation introduced the

first lithium-ion batteries in 1990 for its camcorder (Blomgren, 2016). Lithium-ion possess many advantages as compared to its fellow competitors in the market and being marketed worldwide. LIB have become the clean alternative and also being widely use in the automotive industry as the replacement of fuel driven engine. These battery-powered vehicles are known as electric vehicles (EV) and has obtained worldwide recognition due to its clean and environmentally friendly engine.

An electric driven vehicle, or simply known as electric vehicle (EV) is a type of vehicle propelled by a single or multiple electric motors or traction (Flah, Mahmoudi, & Lassaad, 2015). This particular type of vehicle is the most promising avenues to materially reduce automobile contributions to petroleum dependency, air pollution and carbon dioxide emissions (Nanaki & J.Koroneos, 2013). EVs are divided into several types depending on the engine and system use. The different type of technologies is battery electric vehicle, plug-in hybrid electric vehicle, fuel cell electric vehicle and solar electric vehicle.

The main focus of electric vehicle is the battery electric vehicles. It is also known as the all-electric vehicle (AEV) which uses high capacity batteries and electric motor to move the vehicles (Flah, Mahmoudi, & Lassaad, 2015). The concept of battery vehicle is essentially simple as it only consists of electrochemical batteries for energy storage, an electric motor and a controller (Larminie & Lowry, 2003). It derives all the power from its batteries pack or module and has no internal combustion engine and fuel tank. The only way to recharge the batteries is by plugging the vehicle to a charging point. There are number of advantages by using EV as the daily commuter. AEV uses clean electric energy whereby zero emission of greenhouse gas, low operational cost, has possibility to recover energy from regenerative braking and it operates quietly.

Most of the commercialize AEV uses lithium-ion batteries (LIB) as their energy supplier. Some of the famous and popular AEV in the automobile industry are the Mercedes Benz B-Class Electric, Tesla Model S, BMW i3 and many more. All of these AEV uses LIB pack in a module which acts as their fuel alternative system. LIB is arranged accordingly to maximized the electricity produced. LIB was chosen

because of its high energy and power density, light weight, low self-discharge, high recyclability and long-life cycle as compared to other rechargeable batteries such as the nickel-metal hydride (Ni-MH).

Figure 2.1 displayed the components inside the lithium-ion batteries which consists of cathode, anode, electrolyte and separator (Samsung,2016). Lithium-ion batteries are made up of a number of different components. A typical LIB configuration includes a lithium compound-based cathode, a carbon-based anode, an electrolyte, and a separator (Ma, et al., 2018). Based on Ma (2018), cathode materials are coated on an aluminum foil while the anode material are coated on a copper foil. Both of this foil acts as the current collectors. A porous polymer separator that is immersed in the organic salt electrolyte which then being sandwiched between the anode and cathode functions to prevent the shorting of the two electrodes (Ma, et al., 2018).

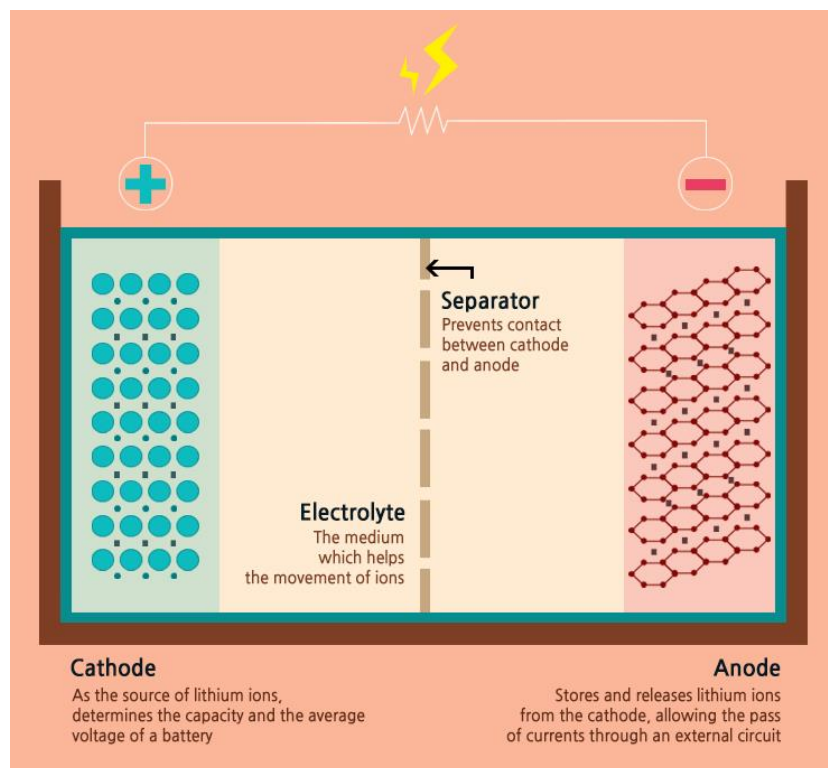


Figure 2.1: Components inside lithium-ion batteries (Samsung,2016)

Lithium-ions go through the cycles of intercalation and deintercalation and passes through the electrolytes whereby the charges carry in the internal circuit (Pender, et al., 2020). Redox reaction occurs at the electrodes by the intercalation and deintercalation of the ions. Electrons are generated by the redox reaction and it moves directionally through the external circuit to form current (Electrolytic Cells, 2020). The movement of ions and electrons in the internal and external circuit respectively creates electricity and becoming the lead operation of LIB (Ma, et al., 2018).

LIB is commonly found in a cylindrical format cell and commercially available cell is the 18650 lithium-ion batteries similar to Figure 2.2. The 18650 LIB dimensions can be obtained from its name literally where it has 18 mm of diameter and 65 mm of length. According to Neverman (2020), the 18650 LIB has a voltage of 3.7 V and has between 1800 mAh and 3500 mAh of capacity with optimum operating temperature of 288.15 K to 308.15 K. Furthermore, the average charging time is about four hours. Due to these exceptional performances, LIB is the most popular option in the electrochemical cell family. Figure 2.2 shows the sizing of lithium-ion batteries which is widely used in and available in the market.



Figure 2.2: Lithium-ion batteries (Samsung,2016)

However, the operation of LIB including discharging and recharging generates heat. The rapid movement of ions and electrons, redox reaction and internal resistance produces heat and excess heat have multiple negative effects on a battery as in Figure 2.3. When the temperature reaches 363.15 K, the Solid Electrolyte Interphase (SEI)

film will start exothermic decomposition on the electrode (Lu, Han, Li, Hua, & Ouyang, 2013). Peled (1979), introduced the concept of SEI as an electronically insulating and ionically conducting passivation layer, formed between the electrode and electrolyte acting as a solid electrolyte. A dense and intact SEI will restrict the electron tunneling thus prohibit further reduction of the electrolyte which is essential for the chemical and electrochemical stability. SEI also consume active lithium and electrolyte materials and able to lead to capacity fading, increasing battery resistance and poor power density (Wang, Kadam, Li, Shi, & Qi, 2018). Increasing battery resistance will bring up the heat due to Joule effect and in extreme cases, a thermal runaway occurs. Figure 2.3 indicates the degradation mechanisms inside lithium-ion batteries due to excess heat (Birkl, Roberts, Mcturk, Bruce & Howey, 2017).

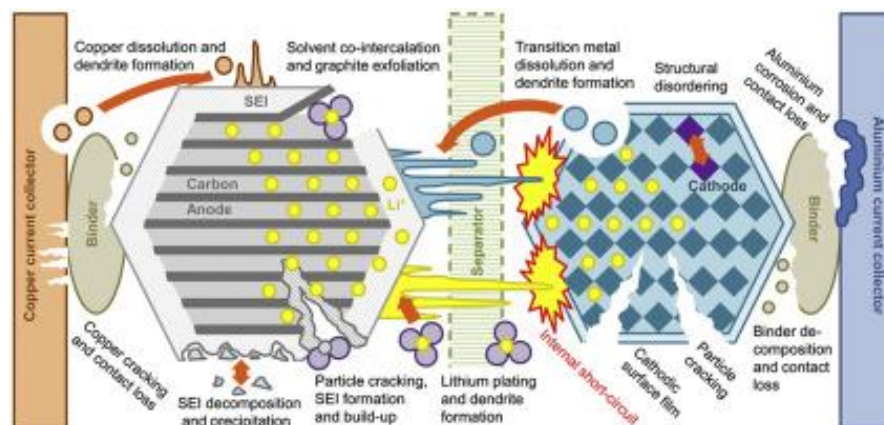


Figure 2.3: Degradation mechanisms inside lithium-ion batteries (Birkl, Roberts, McTurk, Bruce & Howey, 2017)

In order to prevent the battery to degrade due to excessive heat, a battery thermal system have to be designed to remove the detrimental heat to protect the performance and lifespan of the batteries. Battery thermal management system (BTMS) can also be known as the brain of a battery pack. BTMS needed to oversee and manage the copper temperature of batteries, state of charge, voltage protection and cell health monitoring. The ideal design of a BTMS is being able to operate safely and robustly within the restricted space, provided that the necessary heat transfer and be possible to be economically manufactured (Smith, Singh, Hinterberger, & Mochizuki, 2018). BTMS is needed to prevent the buildup of SEI, thermal runaway, power fade, decrease lifespan and efficiency.

A well designed BTMS using proper cooling medium has to be able to cool down the battery by removing all the unwanted heat to promote a safe condition for the cells to operate. There are a number of cooling medium which acts as the coolant for the BTMS such as air, liquid and phase change material. However, BTMS using air is among the best choice due to its lower cost, easy practicality and good cooling performance makes it one of the commercial chosen cooling strategies (Wang & L.Ma, 2017). Figure 2.4 is an example of an air-cooling battery management system commercially used in the industry.

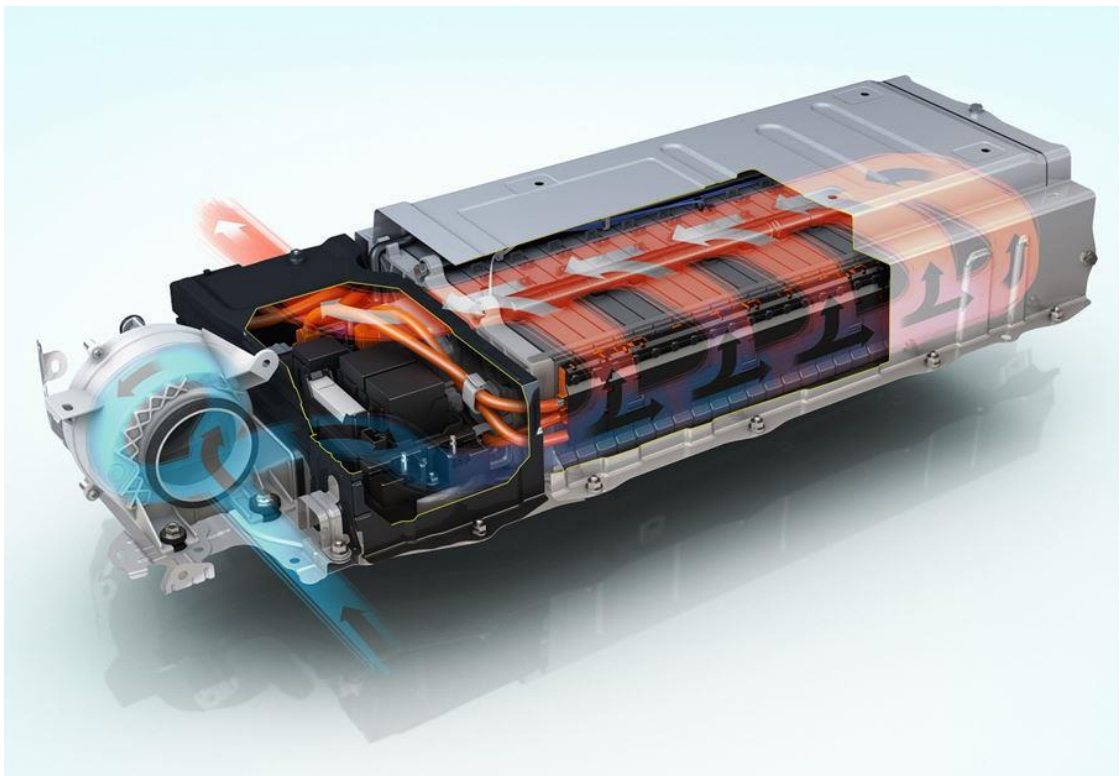


Figure 2.4: Air cooling battery thermal management system (Quesnel, 2018)

CHAPTER 3

METHODOLOGY

This project utilizes COMSOL Multiphysics 5.4 as its main modelling software. Computational Fluid Dynamics (CFD) analysis will be used to study the effect of air as the cooling medium. Cooling strategies parameters such as the arrangement of LIB in a pack, the flow characteristic of air and the air inlet and outlet sizing are design to serve the purpose of great cooling efficiency. The simulation uses 18650 lithium-ion batteries and the temperature of the batteries are also being studied and reviewed in this report. Figure 3.1 shows the methodology flowchart of the simulation work to obtained the best cooling strategies.

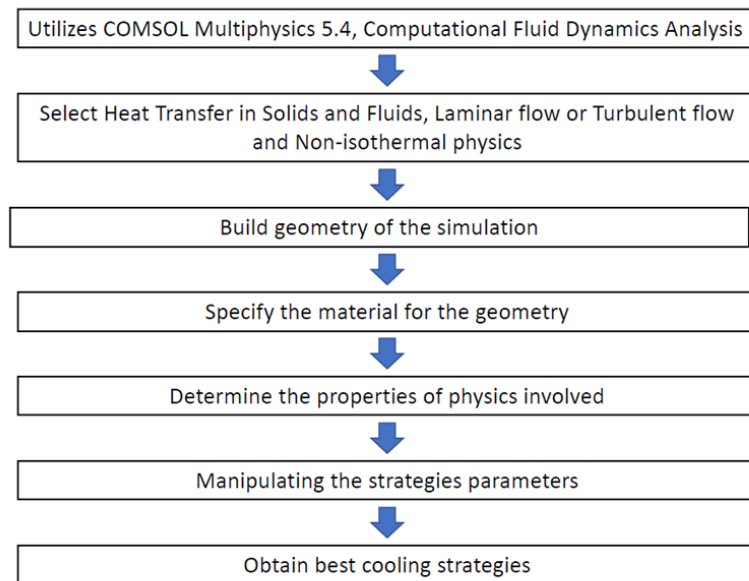


Figure 3.1: Simulation methodology flowchart

3.1. Comparison of Research Method

Choice of methodology is heavily influenced by the research question. A similar research was done by Lu (2018), discussed on the study of forced air-cooling strategy for lithium-ion battery pack (Lu, et al., 2018). However, the research only focuses on the arrangement of the battery pack and the distance between the battery cells and did not cover the manipulating parameters such as air inlet and outlet sizing, type of air flow and velocity of air. Table 3.1 shows the comparison between this paper and Lu's research on air cooling of lithium-ion batteries.

Table 3.1: Comparison of research method

Differences	Parametric study of forced air-cooling strategy for lithium-ion battery pack with staggered arrangement (Lu, et al., 2018)	Cooling Strategies Of Lithium-Ion Batteries Using Air
Arrangement of batteries in a pack	Arrangement is kept constant with stagger-arranged battery. The appropriate distance among the batteries is being studied.	The best layout analysis will be manipulated further. The appropriate distance among the batteries will also be manipulated.
Air inlet and outlet sizing	The coolant inlet and outlet sizing are kept constant to 10 mm.	The coolant Inlet and outlet sizing will be manipulated.
Flow characteristic of air	The airflow is kept constant as steady, incompressible and laminar flow.	The airflow characteristic such as type of flow and velocity of air will be manipulated.

3.2 Project's Modelling Methodology

The battery layout analysis in this research will cover the connection between the batteries either in series or parallel or combination of both connections. The number of batteries proposed in this research is nine therefore proper arrangement is needed to maximize the cooling performance without neglecting the power generation. The distance between the battery cells is also being determined as both of the selection will be further studied as the main configuration.

For the characteristic of air, the type of flow will be manipulated. Both laminar and turbulence flow will be studied to suit the cooling strategies alongside with the air velocity which will also be determined for an effective cooling. The flow of air in the pack will be simulated to ensure air comes into contact with all the batteries thus reducing the overall temperature. The coolant inlet and outlet sizing will be determined to guarantee enough air is coming into the system therefore able to cool down the batteries. All of these parameters will be simulated in COMSOL Multiphysics using the Computational Fluid Dynamics. The simulation will utilize heat transfer in solids and fluids, laminar and turbulent flow, and non-isothermal flow. The manipulation of parameters will be studied to keep the battery within its safe temperature of below 308.15 K.

3.3 COMSOL Multiphysics 5.4 Software

The simulation of the air-cooling process utilizes COMSOL Multiphysics 5.4 software as its main application. The built model was designed in 3D and the chosen study in the simulation was stationary study. The particular reason for this chosen study is to neglect the changes of temperature over time. Furthermore, there were three set of physics being used as part of the simulation. These physics set are converged together with Multiphysics functions as non-isothermal flow. The physics module involved were heat transfer in solids and fluids, laminar flow and turbulent flow.

3.3.1 Heat Transfer in Solids and Fluids

The heat transfer in solids and fluids physics module is used to model the heat transfer by conduction and convection. The conduction heat transfer models the conduction process going on within the heat source and the battery layers. In a continuous medium, Fourier's law of heat conduction states that the conductive heat flux, \mathbf{q} , is proportional to the temperature gradient. In case of a moving fluid, the energy transported by the fluid is modeled in combination of fluid flow and referred to as convection of heat. This particular module includes the descriptions for heat conjugate heat transfer which is the heat transfer in solids and fluids in the same system.

3.3.2 Laminar Flow (spf)

The laminar flow interface is used to compute the velocity and pressure fields for the flow of a single-phase fluids in the laminar flow regime. The physics interface utilizes compressible flow at low Mac number (typically less than 0.3). The equations solved by the laminar flow interface are the Navier-Stokes equations for conservation of momentum and the continuity equation for conservation of mass.

3.3.3 Turbulent Flow, k- ϵ (spf)

The turbulent flow interface is also used to compute the velocity and pressure fields for the flow of a single-phase fluids in the laminar flow regime. The physics interface operates using compressible flow at low Mac number (typically less than 0.3). The equations solved by the turbulent flow interface are the Reynolds-averaged Navier-Stokes (RANS) equations for conservation of momentum and the continuity equation for conservation of mass. Turbulence effects are modelled using the standard two equation k- ϵ model with realizability constraints. The flow near the walls is modeled using wall function.

3.4 Properties of Lithium-Ion Batteries

The lithium-ion battery cell is made up of several layers consisting of cathode, anode, separator and current collectors wound spirally into a cylinder. These different layers have different thermal physical properties such as their thermal conductivity, specific heat capacity and density. Nevertheless, the detailed structure of the battery has very low significance on the impact of battery's thermal performance (Peng,2020). The heating of the battery during discharging also varied depending on the discharge rate. Hence, to simplify the simulation model and to keep the accuracy of the results as well, a single lithium-ion battery is considered as a homogenous cylinder defined as a lumped model with a heating source in the middle with the given properties as in Table 3.2. Based on the heat source power, the temperature of the batteries without cooling is at 350 K, therefore cooling strategies are needed to keep the batteries within its safe operating temperature.

Table 3.2: Properties of lithium-ion batteries

Properties	Value
Density (kg/m ³)	2812.7
Thermal conductivity (W/m.K)	141.2
Specific heat capacity (J/kg.K)	922.4
Nominal voltage (V)	3.6
Number of batteries	9
Heat source (W/m ³)	1468788.25
Temperature of batteries (K)	350
Battery length (m)	0.065
Battery diameter (m)	0.09
Heat source length (m)	0.065
Heat source diameter (m)	0.02

3.5 Properties of Air

The coolant selected for this research is air due to its structure simplicity, light weight, low cost and has a good cooling performance (Wang & L.Ma, 2017). The properties of air are prespecified according to the material content values constant stored by COMSOL Multiphysics software. The properties of air such as temperature, density, ratio of specific heat, mean molar mass and some other properties which are temperature dependent were kept constant throughout the simulation process. Both laminar and turbulent flow will utilize the same properties of air to neglect the air variance for both manipulated flows. The properties of air used in the simulation work are given in Table 3.3.

Table 3.3: Properties of air

Properties	Value
Temperature (K)	293.15
Ratio of specific heat	1.4
Density (kg/m ³)	1.225
Mean molar mass (kg/mol)	0.02897

3.6 Boundary and Initial Condition

The initial simulation model consists of 9 cylinders representing the properties of lithium-ion battery. The heat source is placed in the middle of every cylinder to indicate the heat within the battery. The batteries are initially arranged in 3S3P (3 cells in series and 3 cells in parallel). The spacing between each battery is set at 0.001 m in both x and y axis. The air is simulated by the block with an initial inlet and outlet opening of 0.065 m while the remaining boundaries are set as symmetry.

The air inlet also known as the inflow is set to be velocity boundary condition while the outlet which is outflow is set to be pressure boundary condition with normal flow and suppress backflow conditions. The project focuses on the cooling strategies of lithium ion battery therefore, the battery holder alongside with the circuit connection

were neglected to keep the project well within its objectives. Figure 3.2 shows the simplified geometry of the 3D simulation model.

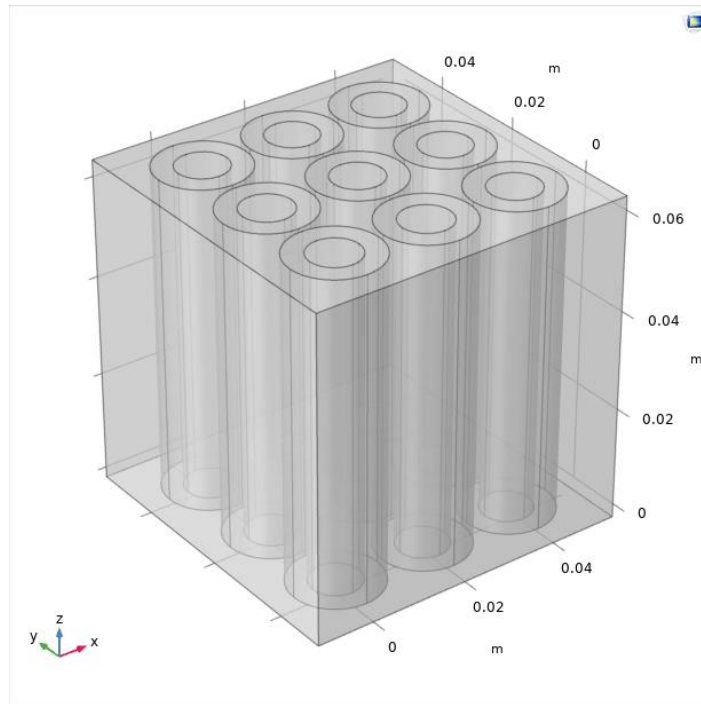


Figure 3.2: 3D simulation model

3.7 Meshing Numerical Scheme

The simulation model is built in 3D can be mesh into several types of meshing element size available in COMSOL Multiphysics software. The chosen sequence type of the mesh is physics-controlled mesh with physics contributor from the heat transfer in solids and fluids, laminar or turbulent flow and the Multiphysics of non-isothermal flow. Three meshing element size were being tested for this 3D simulation model namely coarse mesh (107138 domain elements), normal (170659 domain elements) and lastly fine (340165 domain elements). The design properties and parameters of the model are kept constant for all the tests to obtain accurate results. The design properties and parameters of the model are displayed based on Table 3.4.

Table 3.4: Design properties and parameters of 3D model

Parameters	Value
Batteries layout	3S3P
Distance between batteries, x and y axis (m)	0.001
Air inlet and outlet sizing (m)	0.065
Type of flow	Laminar flow
Velocity of air (m/s)	2.00

The meshing tests were conducted to study the effect of meshes element size along the x direction with the location of y is constant at 0 m and z is constant at 0.0325 m. Figure 3.3 shows the evolutions of temperature along the x-axis for all three tests.

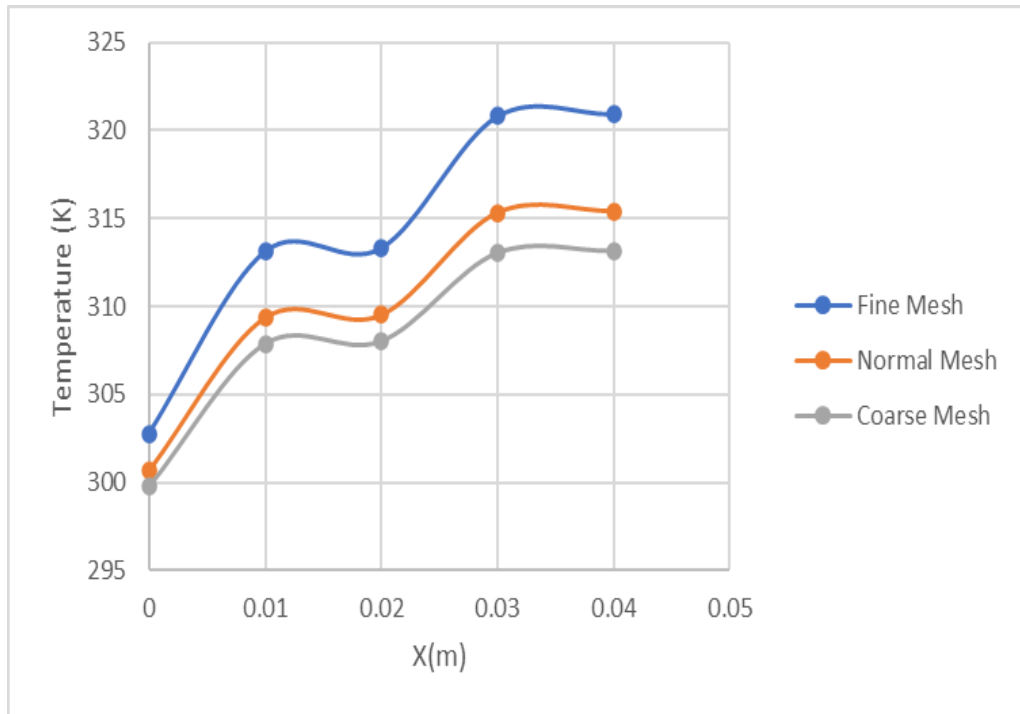


Figure: 3.3: Temperature evolution along the x-axis for all types of meshes

As can be seen from Figure 3.3, the temperature evolution difference for all three types of meshes is quite significant. Coarse mesh recorded the lowest maximum temperature of 313.13 K while normal mesh recorded a maximum temperature of 315.42 K. The most refined mesh type recorded a maximum temperature of 320.96 K as the greater the number of domain elements, the more grid being tested.

Therefore, to keep the result as accurate as possible and to obtain a reliable finding, fine mesh is chosen as the main mesh for the simulation. Figure 3.4 shows the chosen mesh of fine mesh with domain elements of 340165.

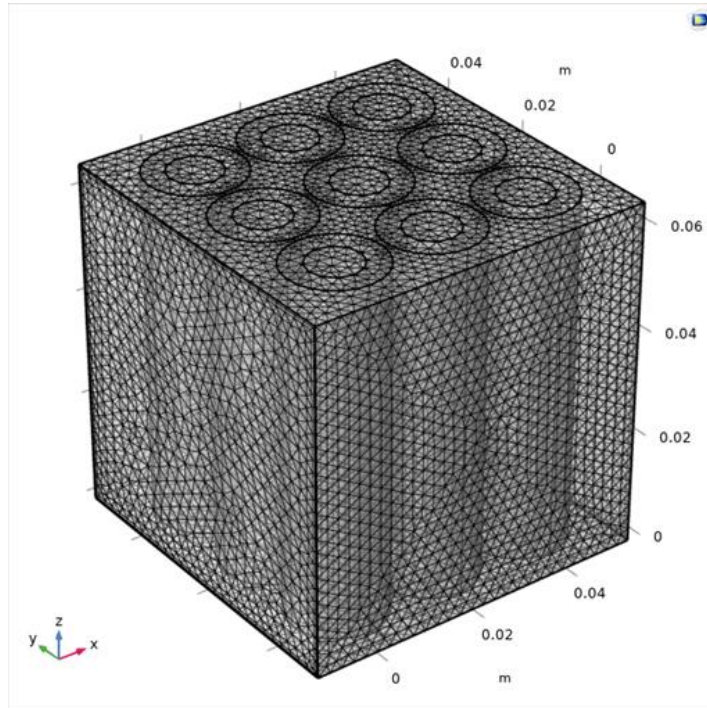


Figure 3.4: Fine mesh simulation model

CHAPTER 4

RESULT AND DISCUSSION

One of the objectives of this research is to evaluate important parameters which affect air cooling effectiveness. The parameters being evaluated are the battery layout analysis, distance between the battery cells, air inlet and outlet sizing, type of flow and velocity of air will all be evaluated within this part of the paper. The working lithium-ion batteries used in this research has a power volume of 1468788.25 W/m^3 with a temperature of 350 K with 0 m/s velocity of air (stagnant air). By manipulating and evaluating all of the parameters, the goal of the simulation is to reduce the high working temperature of the batteries to its' safe optimum operating temperature of 288.15 K to 308.15 K.

4.1 Battery Layout Analysis

All of the lithium-ion batteries were arranged vertically for this battery layout analysis. An initial layout of three batteries in series and three batteries in parallel was tested to validate the simulation model making sure the model is able to converge. Next, two best possible layouts being considered and tested in this project which are three batteries in series and three batteries in parallel (3S3P) and nine batteries in series (9S). were simulated. Figure 4.1 shows the simulation model of the 3S3P batteries layout while Figure 4.2 shows the simulation model of the 9S batteries.

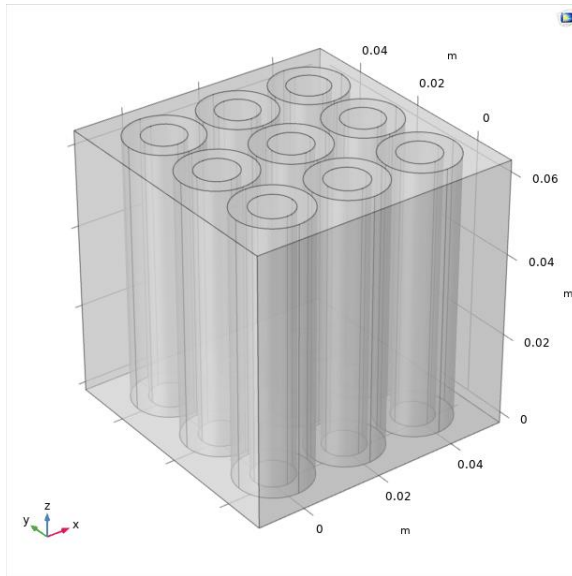


Figure 4.1: 3S3P batteries layout

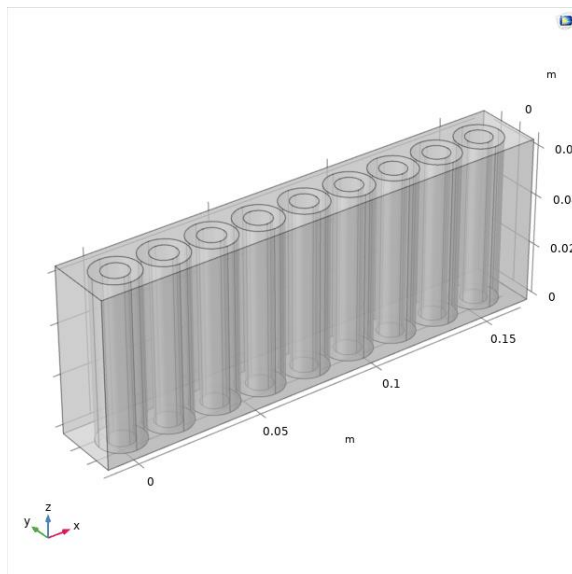


Figure 4.2: 9S batteries layout

To extensively compare the advantages and disadvantages between these two layout configurations, only a single variable is being monitored to make a comparative analysis. The temperature distribution of the battery was being measured by keeping other parameters constant. Figure 4.3 shows the temperature distribution in 3S3P batteries layout while Figure 4.4 shows the temperature distribution in 9S batteries layout.

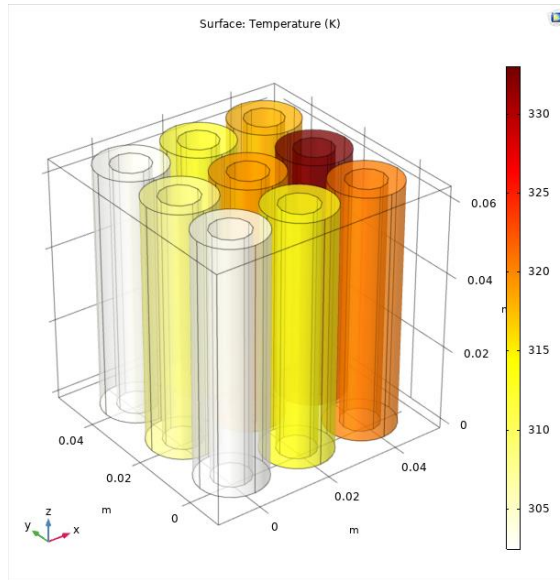


Figure 4.3: Temperature distribution in 3S3P batteries layout

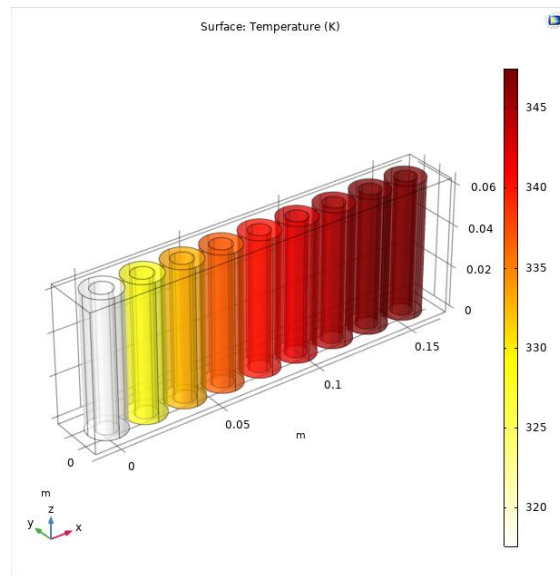


Figure 4.4: Temperature distribution in 9S batteries layout

Based on Figure 4.3, it can be observed that the temperature distribution for 3S3P batteries layout configurations after the cooling process is better as compared to the 9S batteries layout as in Figure 4.4. The cooling is more uniform in the mixed setup rather than the straight-line series connection. As recorded in Table 4.1, the highest temperature recorded among the batteries in the 3S3P layout is 332.98 K and its average temperature is just 314.67 K while for the 9S layout highest temperature and average temperature is recorded at 347.49 K and 337.37 K respectively. This result is due to the flow of air being able to reach the surface of the batteries more for the 3S3P

layout causing the temperature to decrease in contrast to the 9S layout. In the 9S layout, the air is not distributed evenly as can be proven by the temperature gradient bar chart in Figure 4.5, where the maximum temperature is just shy of the initial temperature of 350 K to 347.49 K thus manifesting inefficient cooling. The maximum temperature is obtained on the 9th battery which is located at the end of the layout, moving further along the x-axis.

Table 4.1: Temperature distribution for 3S3P and 9S batteries layout

Layout Arrangement	T_{\max} (K)	T_{avg} (K)
3S3P	332.98	314.67
9S	347.49	337.37

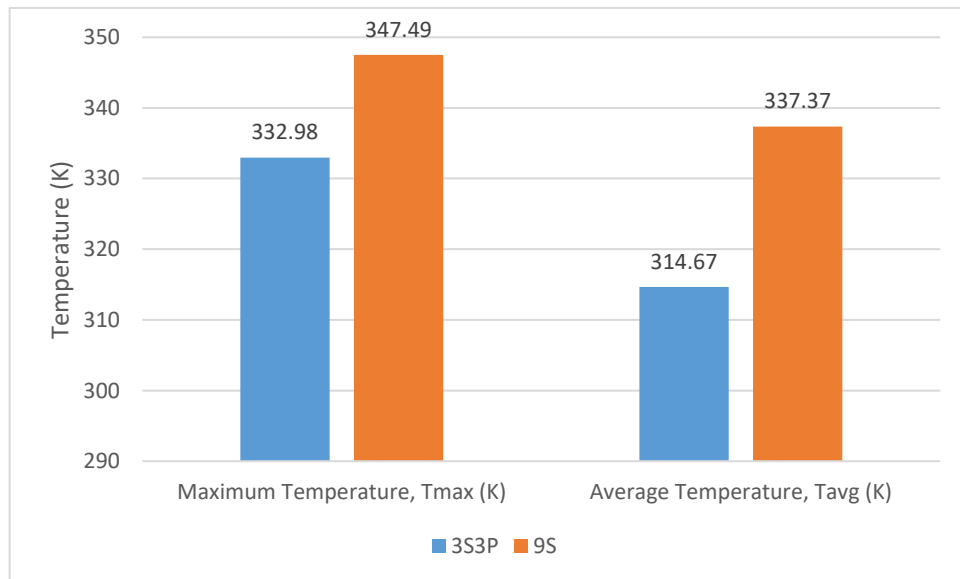


Figure 4.5: Temperature differences for 3S3P and 9S batteries layout

Therefore, according to the findings, 3S3P has been proven to become the best battery layout as the heat transfer to the coolant perform better and the cooling is more homogenous as compared to the 9S setup.

4.2 Distance between battery cells

The distance between the cells plays an important role in the cooling strategies. The coolant has to be in contact with all the cells to obtain uniform cooling. As recorded in Table 4.2 and Figure 4.6, there were three tests being conducted with different distance in terms of x and y axis and the temperature distribution were being examined. The air velocity alongside with air inlet and outlet were kept constant based on the best layout arrangement. Similarly, the air flow will be in x-direction as the horizontal coolant direction. The maximum distance between the cells were kept within the sizing of the air channel for both axes to maintain the compactness of the battery pack and enhance the space utilization.

Table 4.2: Temperature distribution for different distance between the battery cells

Distance between batteries (x and y axis)	T_{\max} (K)	T_{avg} (K)
0.001 m	332.98	314.67
0.002 m	313.75	306.99
0.003 m	309.13	305.29

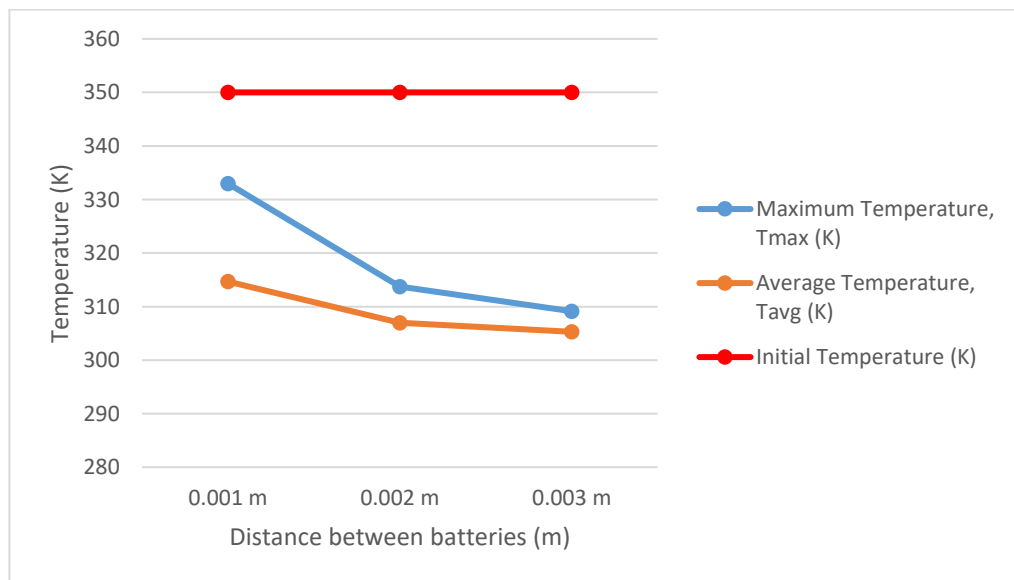


Figure 4.6: Temperature vs Distance between the batteries graph

The light of the outcome based on Table 4.2 and Figure 4.6, proves that the distance between each battery is very crucial to determine the cooling strategies. As

the distance between the batteries increase, the recorded maximum temperature decreases rapidly based on Figure 4.6. For the distance of 0.001 m, the maximum temperature is 332.98 K and reduces swiftly to 309.13 just by increasing the distance by 0.002 m. The larger the distance between the cells, the more coolant can pass through each of them thus creating a better cooling performance. As shown by Figure 4.7, good cooling performance where the temperature of the batteries in the third column which is at the end row of the battery pack is significantly reduced by the parameters studied in this simulation.

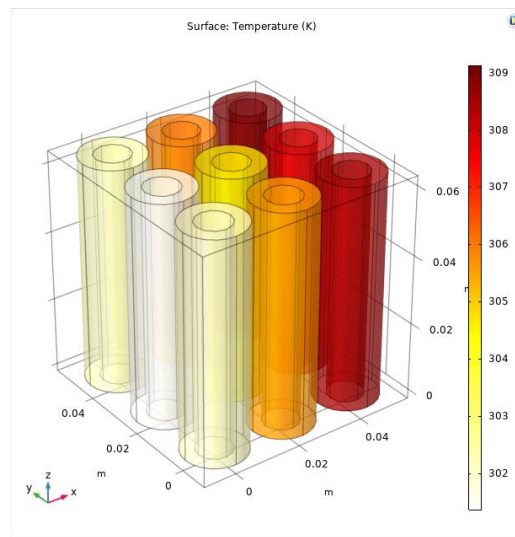


Figure 4.7: Temperature distribution for 0.003 m distance between the battery cells

The simulation focuses on the second row of the battery pack as it resulted in the highest temperature among the rows due to the screening of air. Figure 4.8 shows the plot of the said second row while Figure 4.9 shows the temperature in the middle of the three batteries. Based on the graph seen from Figure 4.9, the temperature of the middle row batteries decreases rapidly for the distance of 0.001 m to 0.003 m. Again, this is due to the ability of coolant to come into contact with the surface of the batteries thus giving a good cooling performance. The mission to obtain the optimum operating temperature below 308.15 K is achievable due to proper spacing between the batteries. Therefore, the distance between the battery of 0.003 is selected to be used in the next parameters.

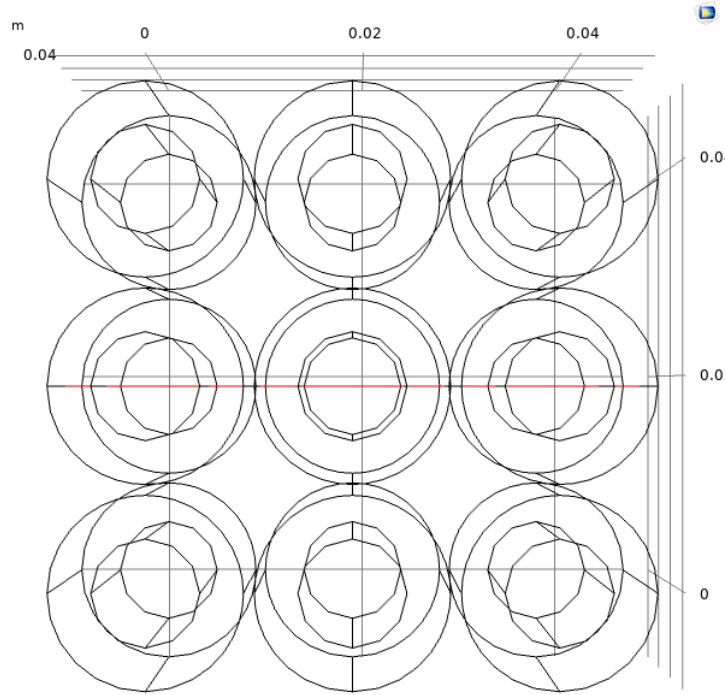


Figure 4.8: Plot of the middle row's batteries

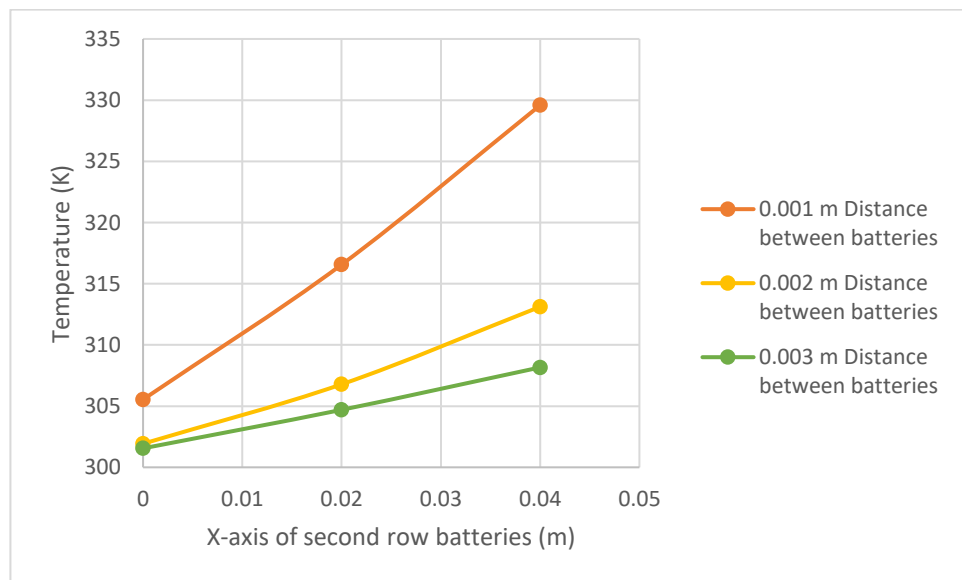


Figure 4.9: Temperature in the middle of middle row batteries for different distance between batteries

4.3 Air Inlet and Outlet Sizing

The coolant enters the battery pack coming into contact with the batteries by a single inlet and an outlet. The inlet of the battery pack is set to a velocity boundary condition while the outlet is set to pressure boundary condition. In this part of the report, the air channel dimension will be manipulated to observed the changes in temperature of the battery thus to inspect the cooling performance. The inlet and outlet sizing focusing on the width will be manipulated accordingly based on Table 4.3, where three tests are conducted with different sizes of the variable. However, the air inlet and outlet sizing are kept below 0.08 m to maintain the compactness of the battery pack and enhance the space utilization. The distance between the battery, air velocity, the flow characteristic will all be kept constant to verify the cooling strategy. The nine lithium-ion batteries are maintained in the middle of the battery pack. Table 4.3 and Figure 4.10 recorded the result for all three-air inlet and outlet sizing tests.

Table 4.3: Temperature distribution for different air inlet and outlet sizing

Air inlet and outlet sizing (m)	T_{\max} (K)	T_{avg} (K)
0.065	309.13	305.29
0.070	314.77	309.19
0.075	321.52	312.76

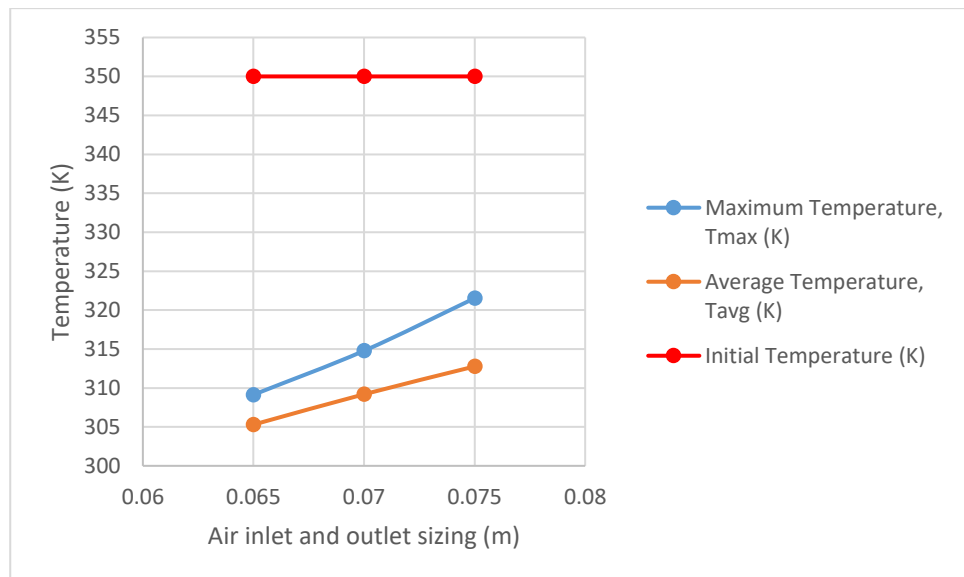


Figure 4.10: Temperature vs Air inlet and outlet sizing graph

In view of the results obtained in Table 4.3 and Figure 4.10, the increment of the air inlet and outlet sizing contributes to a worse cooling performance. The maximum temperature for the maximum air inlet and outlet sizing was among the highest yet recorded for all the parameters. The particular reason behind this result is because the bigger the opening of the inlet and outlet, there is more space for air to escape from the small channel between the batteries leading to poor cooling performance. The air is not trapped among the batteries thus less heat transfer is executed. Thus, the air inlet and outlet sizing will remain the same as before which is at 0.065 m for both of the inlet and outlet.

4.4 Type of Air Flow

The type of air flow is being determined in this part of the research. There were two types of flow being studied and simulated to suit the best cooling strategies namely laminar flow and turbulent flow. Laminar flow occurs when the fluid flows in parallel layers with no disruption between the layers while turbulent flow is a flow regime categorized by its chaotic property changes (Vapourtec,2021). Laminar flow air will enter the battery pack smoothly passing through the surface of the batteries while turbulent flow will scatter the air within the pack. Laminar air flows in a relative straight line and being partially deflected by the curve of the batteries. On the other hand, air begins to scatter around at the beginning or opening of the battery pack hitting the batteries aggressively for turbulent flow. Both of these flows were tested and the temperature distribution of the batteries were being recorded. Table 4.4 and Figure 4.11 indicates the result of the type of flow on the temperatures of the batteries.

Table 4.4: Temperature distribution for different type of air flow

Type of air flow	T _{max} (K)	T _{avg} (K)
Laminar flow	309.13	305.29
Turbulent flow	326.57	317.69

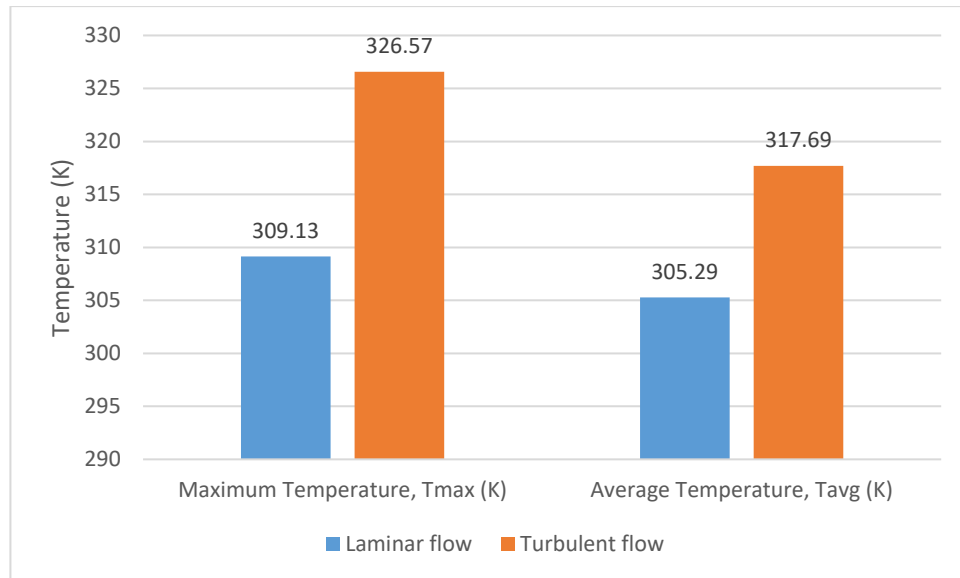


Figure 4.11: Temperature differences for laminar flow and turbulent flow

Having regard to the result obtained from Table 4.4 and Figure 4.11, it is observed that turbulent flow is capable to cool down the batteries but not up to the optimum operating temperature. Laminar flow of compressible air managed to perform better in terms of the cooling performance. This is due to the smooth air flow being able to flow in between the spacing of the batteries and transfer heat between the two mediums. As a result, laminar flow reigns over turbulent flow with an exceptional cooling result.

4.5 Velocity of Air

The last parameters being studied in this project is the air's velocity. All the way through, the simulation was converged by keeping the velocity of air at a constant rate of 2 m/s. The air speed will be further modified to fit in the cooling strategies to cool down the cells alongside with all the parameters such as 3S3P batteries configuration with laminar air flow, having spacing of 0.003 m between the batteries and 0.065 m width and height of the air inlet and outlet. The speed of air is manipulated into 5 different velocity ranging from 2 m/s and up to 10 m/s. Table 4.5 and Figure 4.12 represent the data obtained from the simulation pertaining to the result of difference in air speed.

Table 4.5: Temperature distribution for different velocity of air

Velocity of air (m/s)	T_{\max} (K)	T_{avg} (K)
2	309.13	305.29
4	301.30	299.24
6	298.55	297.17
8	297.16	296.11
10	296.31	295.47

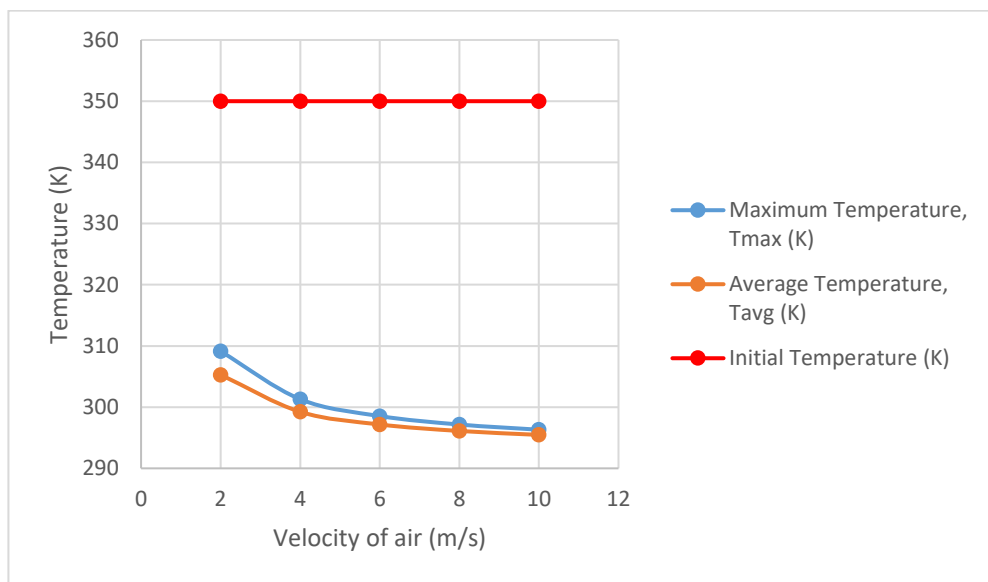


Figure 4.12: Temperature vs Velocity of air graph

Taking account of the result obtained in Table 4.5 and Figure 4.12, the air's velocity is inversely proportional to the maximum temperature. The increase of air's velocity manifests a great cooling performance as just at 6 m/s, both maximum and average temperature is reduced to lower than 300 K. At the maximum velocity of air, the maximum temperature is recorded at 296.31 K which is the lowest obtained temperature throughout the simulation. This decrement of temperature is due to the heat being transfer quickly by the moving air. The faster the air, the faster the heat transfer process going on thus lowering down the temperature quicker.

As before, the main focus once again is at the middle of the battery pack due to the screening of air thus having the highest temperature among the rest. Figure 4.13,

as the velocity increases, the temperature in the middle of batteries also decreases. At 10 m/s speed of air, the highest temperature in the middle of the batteries recorded is 296.09 K. As the result, the velocity of 10 m/s is the chosen velocity to cool down the lithium-ion batteries.

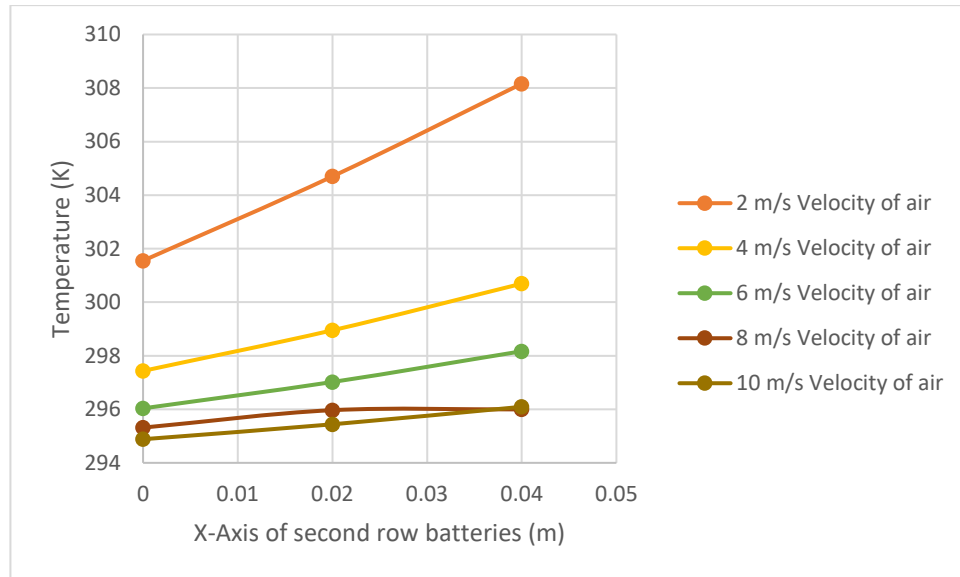


Figure 4.13: Temperature in the middle of middle row batteries for different distance velocity of air

4.6 Best Cooling Strategies

All the parameters had been tested thoroughly to determine the best cooling strategies. The initial temperature of the batteries at 350 K had been cool down rapidly to its' safe optimum temperature of 288.15 K to 308.15 K. The combination of the best cooling strategies resulted in positive decrement of batteries temperature from its initial temperature of 350 K to 296.1 K with the average temperature of the all the batteries of 295.47 K. Table 4.6 accumulates the all the best parameters properties for the best overall cooling strategies.

Table 4.6: Parameters' properties for the best cooling strategies

Parameters	Value/Properties
Battery layout analysis	3S3P
Distance between battery cells	0.003 m
Air inlet and outlet sizing	0.065 m
Type of flow	Laminar flow
Velocity of air	10 m/s

CHAPTER 5

CONCLUSION AND RECOMMENDATION

5.1 Conclusion

Green power is the new energy supplier and will continue to lead the market in the coming future. The dependence of fossil fuel especially in vehicle's engine has been replaced by electrochemical batteries mainly the lithium-ion batteries and have been identified as electric vehicles. However, lithium-ion batteries produce heat when working and the heat generated possess many negative effects towards the performance and lifespan. The batteries have to be kept within its safe operating temperature to avoid any problems from arising due to the heat dissipation. Therefore, cooling strategies had been studied to properly dissipate the heat generated thus to minimize the risk of the worst-case scenario which is thermal runaway. The chosen coolant is air and the cooling strategies parameters were determined in this project. Based on the result of the simulation, the high temperature of 350 K of the batteries were managed to be cooled down to their safe optimum operating temperature of 295.47 K. by having 3S3P batteries layout, 0.003 of distance between the batteries , 0.065 m sizing of air inlet and outlet, a laminar flow of coolant and 10 m/s of air's velocity. All of these parameters have been thoroughly studied to provide the best cooling performance. Therefore, the lithium-ion batteries can be operated safely with these air-cooling strategies of multidisciplinary design optimization.

5.2 Recommendation

The results obtained can become more accurate with a more refined mesh element size. The simulation can be tested by using the most refined mesh which is Extremely Fine mesh to have more domain element thus providing a better result. However, due to the limitation of the computer utilized, the mesh capable to be selected is the fine mesh. Further research is recommended to run the simulation model using Extremely Fine mesh to determine the ultimate best cooling strategies.

To simulate the model to be exactly the same as the commercial battery pack, it is recommended to model the batteries according to the exact properties of the commercially used lithium-ion batteries. The model of the lithium-ion batteries is recommended to be broken down into specific layers and material for each component such as the anode, cathode and so on to visualize the exact lithium-ion batteries thermal properties.

REFERENCES

- Bagotsky, V. S. (2011). Fuel Cells, batteries, and the development of electrochemistry. *Journal of Solid-State Electrochemistry*, 1559-1562.
- Bandhauer, T., Garimella, S., & Fuller, T. (2011). A critical review of thermal issues in lithium-ion batteries. The electrochemical Society.
- Birkl, C. R., Roberts, M. R., McTurk, E., G.Bruce, P., & A.Howey, D. (2017). Degradation diagnostics for lithium ion cells. *Journal of Power Sources*, 373-386.
- Blomgren, G. E. (2016). The Development and Future of Lithium Ion Batteries. *Journal of The Electrochemical Society*.
- Campanari, S., Manzolini, G., & Iglesia, F. (2009). Energy analysis of electric vehicles using batteries or fuel cells through well-to-wheel driving cycle simulations. *J Power Sources*, 464-477.
- Dunn, B., Kamath, H., & Tarascon, J. (2011). Electrical energy storage for the grid: a battery of choices. *Science*, 928-935.
- E, J., Yue, M., Chen, J., Zhu, H., Deng, Y., Zhub, Y., . . . Kang, S. (2018). Effects of the different air-cooling strategies on cooling performance of a lithium-ion battery module with baffle. *Applied Thermal Engineering*, 231-241.
- Electrolytic Cells. (2020, August 16). Retrieved from CHEMISTRY: [https://chem.libretexts.org/Bookshelves/Analytical_Chemistry/Supplemental_Modules_\(Analytical_Chemistry\)/Electrochemistry/Electrolytic_Cells](https://chem.libretexts.org/Bookshelves/Analytical_Chemistry/Supplemental_Modules_(Analytical_Chemistry)/Electrochemistry/Electrolytic_Cells)
- Flah, A., Mahmoudi, C., & Lassaad, S. (2015). Overview of Electric Vehicle Concept and Power Management Strategies.
- Kim, J., Oh, j., & Lee, H. (2019). Review on battery thermal management system for electric vehicles. *Applied Thermal Engineering*, 192-212.
- Larminie, J., & Lowry, J. (2003). *Electric Vehicle Technology Explained*. UK: John Wiley & Sons, Ltd.

- Lu, L., Han, X., Li, J., Hua, J., & Ouyang, M. (2013). A review on the key issues for lithium-ion battery management in electric vehicles. *Journal of Power Sources*, 272-288.
- Lu, Z., Yu, X., Wei, L., Qiu, Y., Zhang, L., Meng, X., & Jin, L. (2018). Parametric study of forced air-cooling strategy for lithium-ion battery pack with staggered arrangement. *Applied Thermal Engineering*, 28-40.
- Ma, S., Jiang, M., Tao, P., Song, C., Wu, J., Wang, J., . . . Shang, W. (2018). Temperature effect and thermal impact in lithium-ion batteries: A review *Progress in Natural Science: Materials International*, 653-666.
- Nanaki, E. A., & J.Koroneos, C. (2013). Comparative economic and environmental analysis of conventional, hybrid and electric vehicles – the case study of Greece. *Journal of Cleaner Production*, 261-266.
- Neverman, A. (2020, July 31). Everything You Need to Know About the 18650 Battery. Retrieved from Common Sense Home: 18650 Battery: <https://commonsensehome.com/18650-battery/>
- Peled, E. (1979). The electrochemical behavior of alkali and alkaline earth metals in nonaqueous battery systems—the solid electrolyte interphase model. *Journal of Electrochemical Society*, 2047-2051.
- Pender, J. P., Jha, G., Youn, D. H., M.Ziegler, J., Andoni, I., J.Choi, E., . . . Mullins, C. B. (2020). Electrode Degradation in Lithium-Ion Batteries. *ACS NANO*, 1243-1295.
- Pesaran, A., Santhanagopalan, S., & Kim, G. (2013). Addressing the Impact of Temperature Extremes on Large Format Li-Ion Batteries for Vehicle Applications. *Proceedings of the 30th International Battery Seminar*. Ft. Lauderdale, Florida.
- Qian, Z., Li, Y., & Rao, Z. (2016). Thermal performance of lithium-ion battery thermal management system by using mini-channel cooling. *Energy Conversion and Management*, 622-631.
- Rahman, S. (2003). Green Power: What is it and where can we find it? *IEEE Power & Energy*, 30-37.

- Rowlands, I. H., Parker, P., & Scott, D. (2002). Consumer perceptions of "green power". *Journal of Consumer Marketing*, 112-129.
- Sasaki, T., Ukyo, Y., & Novak, P. (2013). Memory effect in a lithium-ion battery. *Nature Materials*, 569-575.
- Sharaf, J. (2013). Exhaust Emissions and Its Control Technology for an Internal. *International Journal of Engineering Research and Applications*, 947-960.
- Smith, J., Singh, r., Hinterberger, M., & Mochizuki, M. (2018). Battery thermal management system for electric vehicle using heat pipes. *International Journal of Thermal Sciences*, 517-529.
- Tarascon, J., & Armand, M. (2010). Issues and challenges facing rechargeable lithium batteries. *Materials for Sustainable Energy*, 171-179.
- Thomas, K., & J.Newman. (2003). Thermal modeling of porous insertion electrodes. *Electrochemical Society*, 176-192.
- Vidadili, N., Suleymanov, E., Bulut, C., & Mahmudlu, C. (2017). Transition to renewable energy and sustainable energy development in Azerbaijan. *Renewable and Sustainable Energy Reviews*, 1153-1161.
- Wang, A., Kadam, S., Li, H., Shi, S., & Qi, Y. (2018). Review on modeling of the anode solid electrolyte interphase (SEI) for lithium-ion batteries. *Computational Materials*.
- Wang, H., & L.Ma. (2017). Thermal management of a large prismatic battery pack based on reciprocating flow and active control. *International Journal of Heat Mass Transfer*, 296-303.
- Wang, Q., Ping, P., Zhaou, X., Chu, G., Sun, J., & Chen, C. (2012). Thermal runaway caused fire and explosion of lithium ion battery. *Journal of Power Sources*, 210-224.
- Zarnikau, J. (2003). *Energy Policy*. Consumer demand for 'green power' and energy efficiency, 1661-1672.

